

000
001
002
003
004
005

Lung Disease Classification - Applied AI Progress Report

Group-Q

006 Abstract

026 1. Introduction-1.5

Early diagnosis of respiratory diseases like pneumonia and COVID-19 leads to decreased mortality rate [7] and is a powerful way to manage a pandemic [38]. These diseases can be diagnosed using a variety of tests like pulse oximetry, chest x-ray, CT scan [29], PCR [1] however chest X-rays are by far the most accessible [9]. Furthermore, the scan is available in minutes making it one of the fastest ways of diagnosis [30]. However, the bottleneck with this method is the need for an expert radiologists to evaluate the scan [20]. Many researchers have tried to solve this problem using deep learning [34] but haven't been able to come up with models that can replace radiologists. Small [12] and highly imbalanced data [34], along with varying specifications of X-ray scanners are the biggest problems [26] that researchers have faced. Another issue with using deep neural networks in medical settings is its black-box nature [3], doctors and patients will not trust a model that cannot explain its results [21].

This project is an attempt to compare three backbone architectures namely, ResNet-34, MobileNet V3 Large and EfficientNet B1 along with three lung disease datasets to identify the type of architecture that works best for lung disease classification. The small dataset problem and the issue of different radiographic contrast [22] is mitigated using data augmentation. Im-

Figure 1. Effect of pre-processing on Chest X-ray images.

balanced data problem is handled by undersampling the majority class. F1 scores and loss have been used to compare models and select the best overall model. This model has then been used to perform transfer learning and evaluate the improvement over the models trained from scratch. Further, an ablation study was performed on the best model to find the best learning rate. Finally, GradCAM and T-SNE were used to visualize models and understand model predictions better.

Related Works: Test

2. Methodology-2

In this study, 12 models, four for each of the three datasets will be trained. The first three models will be trained from scratch and the fourth model will be trained using transfer learning. The hyperparameters will be fixed across models to produce comparable results. Next, hyperparameters will be tuned to find the best model. Finally, the models will be visualized using t-SNE and Grad-CAM [11] to explain model results. Before training, the images were pre-processed using histogram equalization and Gaussian blur with a 5x5 filter as Gielczyk *et al.* [10] showed that this improved the F1 score by 4% for chest X-ray classification. Visually, the contrast of the scan improved and allowed irregularities to stand out as shown in Fig. 1. Next, the scans were divided into train, validation and test with the 70:15:15 split. During training, images were augmented using RandomHorizontalFlip, RandomAdjustSharpness, and RandomAutocontrast in Pytorch [24] to increase the number of images the model gets to learn from. To train the model, cosine annealing with warm restarts [19] was used along with the Adam optimizer [18] and the cross entropy loss function.

Datasets: (Tab. 1) with varying disease types were chosen to ensure model robustness. Other criteria included the *number of images per class* and *image quality*.

1



Figure 2. Sample images of Chest X-rays.

Dataset	No. of Images	Classes	Size
COVID [5, 6, 25]	10k:3.6k:1.3k	3	299 ²
Pneumonia [17, 33]	3k:1.5k:1.5k	3	224 ²
Chest X-Ray8 [35, 36]	7.2k:7k:7k:4.1k :3.9k:3.5k:2.9k	7	1024 ²

Table 1. Shortlisted Datasets.

Arch.	Params (Mil.)	Layers	FLOPS (Bil.)	Imagenet Acc.
MobileNet	5.5	18	8.7	92.6
EfficientNet	7.8	25	25.8	94.9
Resnet	21.8	34	153.9	91.4

Table 2. Shortlisted Backbone Architectures.

ity as noisy scans can lead to mis-diagnosis [28]. The **COVID** dataset was created using 43 [8] different publications. [5, 6, 25] X-rays with widespread, hazy, and irregular ground glass opacities are of the COVID-19 class [16]. Whereas, the ones with haziness only in the lower regions [39] are viral pneumonia cases as shown in Fig. 2. The **Pneumonia**, dataset contains scans from pediatric patients. [17, 33] Scans with one white condensed area affecting only one side of the lungs are tagged bacterial pneumonia [2]. X-rays which show bilateral patchy areas of consolidation are classified as viral pneumonia [13]. **Chest X-ray 8** dataset was released by NIH [37] with over 100k chest X-ray images and their radiological reports which Wang *et al.* [35] used to create disease labels through NLP. [36] It contains 15 classes but only 7 were chosen for this study. Furthermore, normal class images were undersampled to choose only one scan per patient.

Backbone Architectures: (Tab. 2) of various configuration and blocks were chosen. Other selection criteria were the *number of trainable parameters*, important as total training time and hardware resources are limited for this project and the *top 5 classification accuracy* on the ImageNet 1K benchmark dataset. **ResNet 34:** residual learning network with 34 layers that are made possible by skip connections. The 34

layer variant was chosen to decrease training time. [14] **MobileNet V3 Large:** uses depthwise separable convolution from MobileNet V2 [27] along with squeeze-excitation blocks in residual layers from MnasNet [31]. Howard *et al.* [15] also used network architecture search to find the most effective model. The large configuration was chosen to not compromise on the prediction accuracy. **EfficientNet B1:** uses compound scaling to scale the model by depth, width and resolution. The B1 version was chosen to have faster training without compromising on the accuracy. [32]

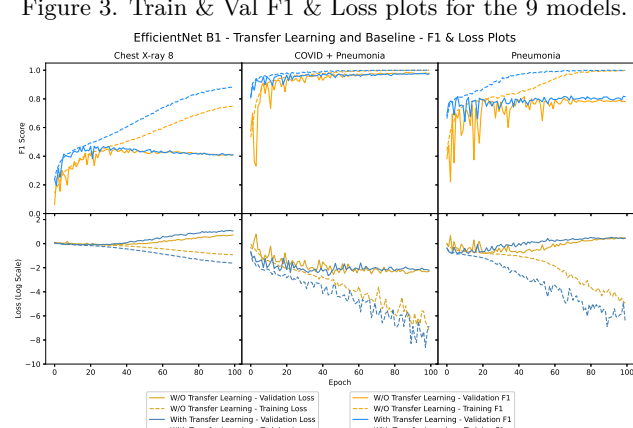
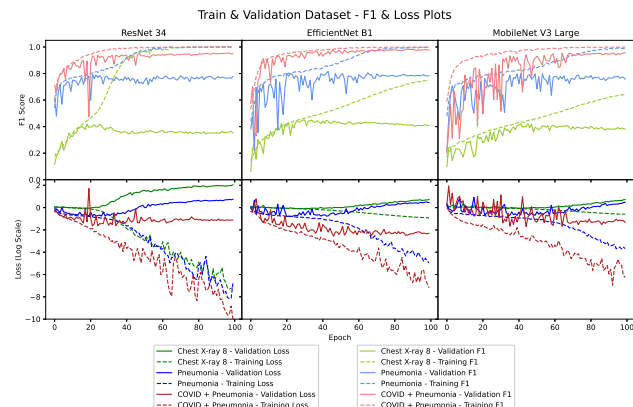
3. Results-2.5

Two datasets in this study had a very small number of samples which caused the models to overfit early. To mitigate this, random contrast and sharpness adjustment [23] data augmentation techniques were used. Some scans in the datasets were anterior-posterior while some others were posterior-anterior and using the horizontal flip data augmentation would make the model invariant to these differences [4]. Inception was the first model trained and each epoch took over 1 hour. To reduce the training time, the X-ray images were resized, pre-processed and split into train, test and validation sets separately. Furthermore, EfficientNet, MobileNet and ResNet 34 were chosen as they have a considerably low number of learnable parameters. Now each epoch is taking less than 4 minutes.

Nine models were trained from scratch and the training, validation F1 score and loss can be seen in Fig. 3. From the plots it is clear that going from a smaller architecture to a bigger architecture, makes the model start to overfit earlier. Another interesting observation is that cosine annealing impacted the loss of MobileNet the most every 10 epochs due to warm restarts. From the graphs it can be seen that all three datasets had similar performance across models when trained for a high number of epochs. The X-ray 8 dataset performed the worst among the three datasets which could be due to the high number of classes as compared to the other datasets. Surprisingly, the pneumonia dataset performed worse than the COVID + pneumonia dataset which indicates that COVID cases are easier to distinguish from pneumonia cases.

216	Model	ResNet			MobileNet			EfficientNet			EN - Transfer Learning			270
217	Dataset	F1	Time	Epoch	F1	Time	Epoch	F1	Time	Epoch	F1	Time	Epoch	271
218	Pneumonia	0.784	82.02	22	0.804	75.49	42	0.768	110.06	44	0.782	114.07	70	272
219	COVID	0.963	67.64	71	0.959	45.90	82	0.970	79.75	89	0.978	56.46	46	273
220	X-Ray 8													274

221 Table 3. F1 (higher is better), time per epoch in seconds (lower is better), and number of epochs to reach the best validation
 222 loss (lower is better) for the 12 models that were trained.
 223



324

References

325

326

327

328

329

330

331

332

333

334

335

336

337

338

339

340

341

342

343

344

345

346

347

348

349

350

351

352

353

354

355

356

357

358

359

360

361

362

363

364

365

366

367

368

369

370

371

372

373

374

375

376

377

- [1] Noorullah Akhtar, Jiyuan Ni, Claire Langston, Gail J Demmler, and Jeffrey A Towbin. Pcr diagnosis of viral pneumonitis from fixed-lung tissue in children. *Biochemical and molecular medicine*, 58(1):66–76, 1996.
- [2] How Drugs are Made and Product List. Viral vs. bacterial pneumonia: Understanding the difference. https://www.pfizer.com/news/articles/viral_vs_bacterial_pneumonia_understanding_the_difference, 2020.
- [3] Paul J. Blazek. Why we will never open deep learning’s black box. <https://towardsdatascience.com/why-we-will-never-open-deep-learnings-black-box-4c27cd335118>, 2022.
- [4] Aleksander Botev, Matthias Bauer, and Soham De. Regularising for invariance to data augmentation improves supervised learning. *arXiv preprint arXiv:2203.03304*, 2022.
- [5] Muhammad E. H. Chowdhury, Tawsifur Rahman, Amith Khandakar, Rashid Mazhar, Muhammad Abdul Kadir, Zaid Bin Mahbub, Khandakar Reajul Islam, Muhammad Salman Khan, Atif Iqbal, Nasser Al Emadi, Mamun Bin Ibne Reaz, and Mohammad Tariqul Islam. Can ai help in screening viral and covid-19 pneumonia? *IEEE Access*, 8:132665–132676, 2020.
- [6] Muhammad E. H. Chowdhury, Tawsifur Rahman, Amith Khandakar, Rashid Mazhar, Muhammad Abdul Kadir, Zaid Bin Mahbub, Khandakar Reajul Islam, Muhammad Salman Khan, Atif Iqbal, Nasser Al Emadi, Mamun Bin Ibne Reaz, and Mohammad Tariqul Islam. Covid-19 radiography database. <https://www.kaggle.com/datasets/tawsifurrahman/covid19-radiography-database>, 2021.
- [7] Priya Daniel, Chamira Rodrigo, Tricia M Mckeever, Mark Woodhead, Sally Welham, and Wei Shen Lim. Time to first antibiotic and mortality in adults hospitalised with community-acquired pneumonia: a matched-propensity analysis. *Thorax*, 71(6):568–570, 2016.
- [8] Società Italiana di Radiologia. Covid pneumonia dataset. <https://sirm.org/category/senza-categoria/covid-19/>, 2020.
- [9] Guy Frija, Ivana Blažić, Donald P Frush, Monika Hierath, Michael Kawooya, Lluis Donoso-Bach, and Boris Brkljačić. How to improve access to medical imaging in low-and middle-income countries? *EClinicalMedicine*, 38:101034, 2021.
- [10] Agata Gielczyk, Anna Marciniak, Martyna Tarczewska, and Zbigniew Lutowski. Pre-processing methods in chest x-ray image classification. *Plos one*, 17(4):e0265949, 2022.
- [11] Jacob Gildenblat and contributors. Pytorch library for cam methods. <https://github.com/jacobgil/pytorchGradCam>, 2021.

- [12] Sarra Guefrechi, Marwa Ben Jabra, Adel Ammar, Anis Koubaa, and Habib Hamam. Deep learning based detection of covid-19 from chest x-ray images. *Multimedia Tools and Applications*, 80(21):31803–31820, 2021.
- [13] W Guo, J Wang, M Sheng, M Zhou, and L Fang. Radiological findings in 210 paediatric patients with viral pneumonia: a retrospective case study. *The British journal of radiology*, 85(1018):1385–1389, 2012.
- [14] Kaiming He, Xiangyu Zhang, Shaoqing Ren, and Jian Sun. Deep residual learning for image recognition. In *Proceedings of the IEEE conference on computer vision and pattern recognition*, pages 770–778, 2016.
- [15] Andrew Howard, Mark Sandler, Grace Chu, Liang-Chieh Chen, Bo Chen, Mingxing Tan, Weijun Wang, Yukun Zhu, Ruoming Pang, Vijay Vasudevan, et al. Searching for mobilenetv3. In *Proceedings of the IEEE/CVF international conference on computer vision*, pages 1314–1324, 2019.
- [16] Adam Jacobi, Michael Chung, Adam Bernheim, and Corey Eber. Portable chest x-ray in coronavirus disease-19 (covid-19): A pictorial review. *Clinical imaging*, 64:35–42, 2020.
- [17] Daniel Kermany, Kang Zhang, Michael Goldbaum, et al. Labeled optical coherence tomography (oct) and chest x-ray images for classification. *Mendeley data*, 2(2), 2018.
- [18] Diederik P Kingma and Jimmy Ba. Adam: A method for stochastic optimization. *arXiv preprint arXiv:1412.6980*, 2014.
- [19] Ilya Loshchilov and Frank Hutter. Sgdr: Stochastic gradient descent with warm restarts. *arXiv preprint arXiv:1608.03983*, 2016.
- [20] P Mehrotra, V Bosemani, and J Cox. Do radiologists still need to report chest x rays? *Postgraduate medical journal*, 85(1005):339–341, 2009.
- [21] Aleksandra Mojsilovic. Introducing ai explainability 360. <https://www.ibm.com/blogs/research/2019/08/ai-explainability-360/>, 2019.
- [22] Andrew Murphy. Radiographic contrast. <https://radiopaedia.org/articles/radiographic-contrast>, 2022.
- [23] Loris Nanni, Michelangelo Paci, Sheryl Brahnam, and Alessandra Lumini. Comparison of different image data augmentation approaches. *Journal of Imaging*, 7(12):254, 2021.
- [24] PyTorch. Transforming and augmenting images. <https://pytorch.org/vision/stable/transforms.html>.
- [25] Tawsifur Rahman, Amith Khandakar, Yazan Qiblawey, Anas Tahir, Serkan Kiranyaz, Saad Bin Abul Kashem, Mohammad Tariqul Islam, Somaya Al Maadeed, Susu M. Zughaiier, Muhammad Salman Khan, and Muhammad E.H. Chowdhury. Exploring the effect of image enhancement techniques on covid-19 detection using chest x-ray images. *Computers in Biology and Medicine*, 132:104319, 2021.

- 432 [26] Melissa Rohman. Ai performs poorly when
433 tested on data from multiple health systems.
434 <https://healthimaging.com/topics/artificial-intelligence/ai-poorly-detects-pneumonia-chest-x-rays>, 2018. 1
435
436
- 437 [27] Mark Sandler, Andrew Howard, Menglong Zhu, Andrei Zhmoginov, and Liang-Chieh Chen. Mobilenetv2:
438 Inverted residuals and linear bottlenecks. In *Proceedings of the IEEE conference on computer vision and*
439 *pattern recognition*, pages 4510–4520, 2018. 2
440
441
- 442 [28] Janaki Sivakumar, K Thangavel, and P Saravanan.
443 Computed radiography skull image enhancement using wiener filter. In *International Conference on Pattern*
444 *Recognition, Informatics and Medical Engineering (PRIME-2012)*, pages 307–311. IEEE, 2012. 2
445
446
- 447 [29] Matt Smith. Common lung diagnostic tests. <https://www.webmd.com/lung/breathing-diagnostic-tests>,
448 2022. 1
449
450
- 451 [30] Healthwise Staff. Chest x-ray. <https://www.healthlinkbc.ca/tests-treatments-medications-medical-tests/chest-x-ray>, 2021. 1
452
453
- 454 [31] Mingxing Tan, Bo Chen, Ruoming Pang, Vijay Vasudevan, Mark Sandler, Andrew Howard, and Quoc V Le. Mnasnet: Platform-aware neural architecture search for mobile. In *Proceedings of the IEEE/CVF Conference on Computer Vision and Pattern Recognition*, pages 2820–2828, 2019. 2
455
456
- 457 [32] Mingxing Tan and Quoc Le. Efficientnet: Rethinking model scaling for convolutional neural networks. In *International conference on machine learning*, pages 6105–6114. PMLR, 2019. 2
458
459
- 460 [33] Tolga. Chest x-ray images. <https://www.kaggle.com/datasets/tolgadincer/labeled-chest-xray-images>, 2020. 2
461
462
- 463 [34] Guangyu Wang, Xiaohong Liu, Jun Shen, Chengdi Wang, Zhihuan Li, Linsen Ye, Xingwang Wu, Ting Chen, Kai Wang, Xuan Zhang, et al. A deep-learning pipeline for the diagnosis and discrimination of viral, non-viral and covid-19 pneumonia from chest x-ray images. *Nature biomedical engineering*, 5(6):509–521, 2021. 1
464
465
- 466 [35] Xiaosong Wang, Yifan Peng, Le Lu, Zhiyong Lu, Mohammad Bagheri, and Ronald M Summers. Chestx-ray8: Hospital-scale chest x-ray database and benchmarks on weakly-supervised classification and localization of common thorax diseases. In *Proceedings of the IEEE conference on computer vision and pattern recognition*, pages 2097–2106, 2017. 2
467
468
- 469 [36] Xiaosong Wang, Yifan Peng, Le Lu, Zhiyong Lu, Mohammad Bagheri, and Ronald M Summers. Nih chest x-rays. <https://www.kaggle.com/datasets/nih-chest-xrays/data>, 2017. 2
470
471
- 472 [37] Wang X, Peng Y, Lu L, Lu Z, Bagheri M, and Summers RM. Nih clinical center provides one of the largest
473 publicly available chest x-ray datasets to scientific community. <https://www.nih.gov/news-events-news-releases/nih-clinical-center-provides-one-largest-publicly-available-chest-x-ray-datasets-scientific-community>, 2017. 2
474
475
- 476
477
478
479
480
481
482
483
484
485
- one-largest-publicly-available-chest-x-ray-datasets-scientific-community, 2017. 2
[38] Lizhou Xu, Danyang Li, Sami Ramadan, Yanbin Li, and Norbert Klein. Facile biosensors for rapid detection of covid-19. *Biosensors and Bioelectronics*, 170:112673, 2020. 1
[39] Na Zhan, Yingyun Guo, Shan Tian, Binglu Huang, Xiaoli Tian, Jinjing Zou, Qiutang Xiong, Dongling Tang, Liang Zhang, and Weiguo Dong. Clinical characteristics of covid-19 complicated with pleural effusion. *BMC Infectious Diseases*, 21(1):1–10, 2021. 2